Hydrol. Earth Syst. Sci. Discuss., 12, 4965–4996, 2015
www.hydrol-earth-syst-sci-discuss.net/12/4965/2015/
doi:10.5194/hessd-12-4965-2015

Hydrology and Earth System Sciences
Open Access
Discussions

Rainfall erosivity estimation based on rainfall data collected over a range of temporal resolutions

S. Yin[1,2], Y. Xie[1,2], B. Liu[1,2], and M. A. Nearing[3]

[1]State Key Laboratory of Earth Surface Processes and Resource Ecology, Beijing Normal University, Beijing 100875, China
[2]School of Geography, Beijing Normal University, Beijing 100875, China
[3]USDA-ARS Southwest Watershed Research Center, Tucson 85719, USA

Received: 22 April 2015 – Accepted: 25 April 2015 – Published: 20 May 2015

Correspondence to: S. Yin (yinshuiqing@bnu.edu.cn)

Published by Copernicus Publications on behalf of the European Geosciences Union.

Abstract

Rainfall erosivity is the power of rainfall to cause soil erosion by water. The rainfall erosivity index for a rainfall event, EI_{30}, is calculated from the total kinetic energy and maximum 30 min intensity of individual events. However, these data are often unavailable in many areas of the world. The purpose of this study was to develop models that relate more commonly available rainfall data resolutions, such as daily or monthly totals, to rainfall erosivity. Eleven stations with one-minute temporal resolution rainfall data collected from 1961 through 2000 in the eastern water-erosion areas of China were used to develop and calibrate 21 models. Seven independent stations, also with one-minute data, were utilized to validate those models, together with 20 previously published equations. Results showed that models in this study performed better or similar to models from previous research to estimate rainfall erosivity for these data. Prediction capabilities, as determined using symmetric mean absolute percentage errors and Nash–Sutcliffe model efficiency coefficients, were demonstrated for the 41 models including those for estimating erosivity at event, daily, monthly, yearly, average monthly and average annual time scales. Prediction capabilities were generally better using higher resolution rainfall data as inputs. For example, models with rainfall amount and maximum 60 min rainfall amount as inputs performed better than models with rainfall amount and maximum daily rainfall amount, which performed better than those with only rainfall amount. Recommendations are made for choosing the appropriate estimation equation, which depend on objectives and data availability.

1 Introduction

Soil erosion leads to land degradation and water pollution and also delivers sediment to streams and rivers, which increases the risks for flooding. Great efforts have been made in many parts of the world to reduce soil erosion by implementing biological, engineering, and tillage conservation practices. Soil erosion prediction models are ef-

HESSD
12, 4965–4996, 2015

fective tools for helping to guide and inform soil conservation planning and practice. The most widely used soil erosion models used for conservation planning are derived from the Universal Soil Loss Equation (USLE) (Wischmeier and Smith, 1965, 1978). These models include the Revised USLE (RUSLE) (Renard et al., 1997) and the Chinese Soil Loss Equation (CSLE) (Liu et al., 2007). RUSLE is the official tool used by government conservation planners in the United States. The CSLE was successfully utilized in the first national water erosion sample survey in China (Liu et al., 2013).

These models have in common the rainfall erosivity factor (R), which reflects the potential capability of rainfall to cause soil loss from hillslopes, and which is one of the most important basic factors for the above mentioned models. In its simplest form, the R factor is as an average annual value, calculated as a summation of event-based energy-intensity values, EI_{30}, for a location divided by the number of years over which the data was collected. EI_{30} is defined as the product of kinetic energy of rainfall and the maximum contiguous 30 min rainfall intensity during the rainfall event. It is the basic rainfall erosivity index that was developed by Wischmeier (1958) originally for the USLE, and is still widely used in other erosion prediction models (e.g., RUSLE and CSLE). Wischmeier and Smith (1976) suggested that more than 20 years' rainfall data are needed to calculate average annual erosivity to include dry and wet periods.

The calculation of EI_{30} requires high-temporal resolution rainfall data, typically breakpoint data, which are often unavailable in many regions of the world where rainfall is recorded only at a daily resolution. Efforts to address this problem have been made to develop simpler methods to estimate rainfall erosivity by using daily (Richardson et al., 1983; Yu, 1998; Capolongo et al., 2008), monthly (Arnoldus, 1977; Renard and Freimund, 1994; Yu and Rosewell, 1996; Ferro et al., 1999), or annual rainfall data (Lo et al., 1985; Renard and Freimund, 1994; Yu and Rosewell, 1996; Bonilla and Vidal, 2011). In general, more rainfall data with longer periods of record are available at these time scales than at sub-event temporal resolution. Generally the technique has been to develop a simple empirical relationship using limited breakpoint data and then to extend the analysis to wider areas and longer periods with coarser temporal resolution

HESSD
12, 4965–4996, 2015

rainfall data (Angulo-Martinez and Begueria, 2012; Ma et al., 2014; Ramos and Duran, 2014; Sanchez-Moreno et al., 2014).

Potential future rainfall erosivity due to climate change has also been studied (Zhang et al., 2010; Shiono et al., 2013; Plangoen and Babel, 2014; Segura et al., 2014). Climate change models (Global Circulation Models) do not predict the rainfall for daily, hourly, or sub-hourly time-scales that would be necessary to directly calculate erosivity. Some studies (Nearing, 2001; Zhang et al., 2010; Shiono et al., 2013; Plangoen and Babel, 2014; Segura et al., 2014), therefore, developed simpler methods based on lower temporal resolution rainfall data and then utilized climate model rainfall data as input to these models to conduct studies concerning climate change on rainfall erosivity and soil erosion. There are also studies reporting trends for rainfall erosivity based on longer series of observed breakpoint data in Europe (Verstraeten et al., 2006; Fiener et al., 2013) and the United States (Angel et al., 2005).

Several simpler models for estimating rainfall erosivity from course resolution data have been developed in China in specific areas, including the Loess Plateau (Wang, 1987; Sun, 1990), Fujian Province (Huang et al., 1992; Zhou et al., 1995) and Anhui Province (Wu, 1994). Wang et al. (1995) first developed a series of simplified equations by utilizing several stations located in different areas of China. In China, specifically, the specifications for surface meteorological observations by the China Meteorological Administration (CMA, 2003) have required since 1950s that the maximum 60 and 10 min rainfall amounts, $(P_{60})_{day}$ and $(P_{10})_{day}$ be compiled, hence these data are readily available in China. The measurements were made using siphon-method, self-recording rain gauges. Maximum daily 10 and 60 min rainfall intensities, $(I_{10})_{day}$ and $(I_{60})_{day}$ are easy to calculate from the $(P_{60})_{day}$ and $(P_{10})_{day}$, also.

Other researchers then used data from more stations with longer series of rainfall records to develop erosivity estimation models with event rainfall and the maximum, contiguous 10 min intensity, I_{10}, in an event (Zhang et al., 2002a), daily rainfall and $(I_{10})_{day}$ (Xie et al., 2001), daily rainfall (Zhang et al., 2002b), monthly or annual rainfall (Zhang and Fu, 2003) and hourly rainfall (Yin et al., 2007). Zhang and Fu (2003)

HESSD
12, 4965–4996, 2015

compared five models for estimating annual average rainfall erosivity, including one model using daily rainfall (Zhang et al., 2002b) and four models using monthly or annual rainfall (Zhang and Fu, 2003). They demonstrated that the model using daily rainfall performed best and that there were no significant differences among the other four models. Xie et al. (2015) found that the daily erosivity model with information on $(I_{60})_{day}$ improved the daily EI_{30} index estimation significantly when compared with that using only daily rainfall totals. The multiplication of daily rainfall and maximum $(I_{10})_{day}$ is used often in place of EI_{30}, due to the difficulty in obtaining the breakpoint data (Zhang et al., 2002b; Zhang and Fu, 2003), but availability of the maximum 10 min intensity data.

Renard and Freimund (1994) developed two power law models for the continental United States using average annual rainfall and a Modified Fournier Index reflecting seasonal variation in precipitation. Using data from 29 sites in southeastern Australia, Yu and Rosewell (1996) calibrated the two models developed by Renard and Freimund (1994) and recommended the model using average annual rainfall as input for the estimation of average annual erosivity because of similar model efficiency as compared with the model using the Modified Fournier Index and the ready availability of annual rainfall data.

Other temporal resolutions of erosivity are often required for soil erosion work in addition to average annual erosivity. For example, in the USLE (Wischmeier and Smith, 1965, 1978) and RUSLE (Renard et al., 1997), both average annual erosivity and its seasonal distribution, represented as half-monthly averages, are used. Event or daily erosivity can also be important in soil loss recurrence analyses and non-point source pollution assessment (Kinnell, 2000; Sun et al., 2009).

The objectives of this study were three-fold: (1) calibrate methods of estimating erosivity for time scales ranging from daily to average annual based on different temporal resolutions of rainfall data from 11 calibration stations with one-minute resolution data; (2) compare models in this study with those published in previous research, based on seven independent validation stations using the same data types; and (3) determine the most accurate methods, based on these data, for calculating different time scales

HESSD
12, 4965–4996, 2015

of erosivity when different temporal resolutions of rainfall data are available. Although several studies have been conducted on this topic in the past, no study used as comprehensive a data set collected over this wide geographic area of China to evaluate the wide range of erosivity time scales needed for erosion work, utilizing such a wide range of temporal resolution rainfall data as the independent variable.

2 Data and Methods

2.1 Database

Data collected at 18 stations by the Meteorological Bureaus of Heilongjiang, Shanxi, Shaanxi, Sichuan, Hubei, Fujian, and Yunnan provinces and the municipality of Beijing were used (Fig. 1, Table 1). These stations were distributed over the eastern water-erosion region of China. One-minute resolution rainfall data (Data M) were obtained by using a siphon to collect self-recording rain gauge observations. The data collection period began in 1971 for Wuzhai (53 663) and Yangcheng (53 975) in Shanxi Province and from 1961 for the remaining 16 stations. The data records ended in 2000 for all stations. Quality control of Data M was done to select the best observation years using the more complete data sets of daily rainfall totals, Data D, which were observed by simple rain gauges at the same stations. Data M was compared with Data D on a day-by-day basis, and those days with deviation exceeding a certain criterion were marked as questionable and were not used in this analysis (Wang et al., 2004). The criterion used was that the data were considered good when the absolute deviation between Data M and Data D was less than 0.5 mm when the daily rainfall amount was less than 5 mm and no more than 10 % when the daily rainfall amount was greater than or equal to 5 mm. Data M in the earlier years of record tended to have more days with missing or suspicious observations. These totals of Data M and Data D were compared year-by-year to determine which years could be designated as "effective" years for use in this study, with an effective year having a relative deviation for yearly rainfall amount

HESSD
12, 4965–4996, 2015

of no more than 15 %. There were at least 29 effective years for all 18 stations, and seven stations had effective years of at least 38 years (Table 1). Note that though there were missing data in the information used, Data D was only used for quality control purposes and the data used in the analysis, Data M, were internally consistent in that only the data from effective years were used in all comparisons reported.

Data M were used to calculate the actual event-based EI_{30} values as a function of the calculated kinetic energy and maximum 30 min rainfall intensity. These were treated as observed values and summed to obtain the erosivity factors, R, for daily, monthly (individual month totals), yearly (individual year totals), average monthly, and average annual time scales. Total rainfall depth values were also compiled into the other temporal resolutions of rainfall data, including daily, monthly, yearly, average monthly, and average annual resolutions. For the eight stations in the northern part of China (including stations in Heilongjiang, Shanxi, Shaanxi provinces and Beijing municipality), only the periods from May through September were used because the siphon, self-recording rain gauges were not utilized in the winter to avoid freeze damage. Percentages of precipitation during May through September to total annual precipitation varied from 75.6 to 89.2 % for these eight northern stations. Data M for the full 12 month year were used from the remaining ten stations located in the southern parts of China.

Eleven stations, including Nenjiang, Wuzhai, Suide, Yan'an, Guangxiangtai, Chengdu, Suining, Neijiang, Fangxian, Kunming, and Fuzhou, marked with dots in Fig. 1, were used to calibrate the models (Table 1). The other seven stations, including Tonghe, Yangcheng, Miyun, Xichang, Huangshi, Tengchong, and Changting, marked with triangles in Fig. 1, were used to validate the models.

2.2 Calculation of the R factor at different time scales

Different time scales for erosivity, R, including event, daily, monthly, yearly, average monthly, and average annual, were calculated based on the one-minute resolution data (Data M). EI_{30} (MJ mm ha^{-1} h^{-1}) is the rainfall erosivity index for a rainfall event, where E is the total rainfall kinetic energy during an event and I_{30} is the maximum contiguous

HESSD
12, 4965–4996, 2015

30 min intensity during an event (Wischmeier and Smith, 1978). An individual rainfall event was defined as a period of rainfall with at least six preceding and six succeeding non-precipitation hours (Wischmeier and Smith, 1978). An erosive rainfall event was defined as one with rainfall amounts greater than or equal to 12 mm, following Xie et al. (2012). Using the equation recommended by Foster (2004) for RUSLE2, rainfall storm energies were calculated as:

$$E = \sum_{r=1}^{n} (e_r \cdot P_r) \quad (1)$$

$$e_r = 0.29[1 - 0.72\exp(-0.082 i_r)] \quad (2)$$

e_r is the estimated unit rainfall kinetic energy for the r th minute (MJ ha^{-1} mm^{-1}); P_r is the one-minute rainfall amount for the r th minute (mm); $r = 1, 2, \ldots, n$ represents each 1 min interval in the storm; and i_r is the rainfall intensity for the r th minute, (mm h^{-1}).

Rainfall erosivity for each day, R_{day}, was calculated following the method by Xie et al. (2015). When a day had only one erosive event and this event began and finished during the same day, then

$$R_{day} = E I_{30} \quad (3)$$

When more than one full rainfall event happened during one day, then

$$R_{day} = \sum_{i=1}^{n} E_{event\_i} \cdot (I_{30})_{event\_i} \quad (4)$$

where n is the number of rainfall events during the day, and E_{event_i} and $(I_{30})_{event\_i}$ are the total rainfall energy and the maximum contiguous 30 min intensity, respectively, for the ith event. When only one part of a rainfall event occurred during one day, then

$$R_{day} = E_{day\_d} \cdot (I_{30})_{event} \quad (5)$$

HESSD
12, 4965–4996, 2015

where $E_{\text{day\_d}}$ is the rainfall energy generated by the part of rainfall occurred during the d^{th} day and $(I_{30})_{\text{event}}$ is the maximum contiguous 30 min intensity for the entire event. The remaining situations were calculated by combining Eqs. (4) and (5).

Monthly, yearly, average monthly, and average annual R values were summed from the event EI_{30} index by erosive storms that occurred during the corresponding period. They were calculated by using Eqs. (6)–(9).

$$R_{\text{month},y,m} = \sum_{j=0}^{J} (EI_{30})_{y,m,j} \tag{6}$$

$$R_{\text{ave\_month},m} = \frac{1}{Y} \sum_{y=1}^{Y} R_{\text{month},y,m} \tag{7}$$

$$R_{\text{year},y} = \sum_{m=1}^{12} R_{\text{month},y,m} \tag{8}$$

$$R_{\text{annual}} = \sum_{m=1}^{12} R_{\text{ave\_month},m} \tag{9}$$

where $(EI_{30})_{y,m,j}$ is the EI_{30} value for the jth event in the mth month of the yth year; $R_{\text{month},y,m}$ is the R value for the mth month of the yth year; $R_{\text{ave\_month},m}$ is the average R value for the mth month over the years of record; $R_{\text{year},y}$ is R value in the yth year; and R_{annual} represents average annual erosivity, correspondent to the annual average R-factor in the USLE ($\text{MJ mm ha}^{-1}\,\text{h}^{-1}\,\text{a}^{-1}$).

2.3 Model calibration using different resolutions for rainfall data

A total of 21 models were calibrated for different time scales of R, based on different resolutions of rainfall data (Table 2). Event amount P_{event} and peak intensity indices were derived based on the one-minute resolution data, including I_{10}, I_{30}, and I_{60}, which

HESSD
12, 4965–4996, 2015

were the maximum contiguous 10, 30, and 60 min intensities, respectively, within an event. I_{10} and I_{60} were used because of their close correlation with the daily $(I_{10})_{day}$ and $(I_{60})_{day}$ values commonly reported by the Chinese Meteorological Administration. Four event-based models were developed relating measured EI_{30} to estimated EI_{30} (Table 2). Similar models for the other time scales were also calibrated (Table 2). Data was organized in various ways. P_{day}, P_{month}, P_{year}, P_{ave_month}, and P_{annual} were the daily, monthly, yearly, average monthly, and average annual rainfall amounts, respectively. $(P_{60})_{month}$ and $(P_{60})_{year}$ represented maximum contiguous 60 min rainfall amount observed within a specific month or year, respectively. $(P_{60})_{month\_max}$ represented the maximum of all $(P_{60})_{month}$ values, or the single maximum contiguous 60 min rainfall amount that occurred in a month (from January through December) over the entire period of record. The average of $(P_{60})_{month}$ values was $\overline{(P_{60})_{month}}$. $(P_{60})_{year\_max}$ was the maximum value of $(P_{60})_{year}$ and $\overline{(P_{60})_{annual}}$ was the average of $(P_{60})_{year}$ values. P_{1440} was daily rainfall amount and its related index, including $(P_{1440})_{month}$, $(P_{1440})_{year}$, $(P_{1440})_{month\_max}$, $\overline{(P_{1440})_{month}}$, $(P_{1440})_{year\_max}$, and $\overline{(P_{1440})_{annual}}$, which were defined in a similar way as those for P_{60}.

The parameters were obtained station-by-station for calibration stations first and parameters for linear relationships were compared to determine if data from all stations could be pooled together to conduct regressions (Snedecor and Cochran, 1989). Parameters for power-law models, including Monthly I, Yearly I, Average Monthly I, and Annual I (Table 2), were obtained by using the Levenberg-Marquardt algorithm (Seber and Wild, 2003). Note that models coded as "Annual" refer to annual averages.

2.4 Models published in previous research for comparison

A total of 20 representative models developed using data from China in previous research were compared (Table 3). For these models other variables were calculated. P_{d12} was average daily erosive rainfall total and P_{y12} was average annual erosive rainfall total. P_{5-10} represents the rainy season rainfall amount from May through October

HESSD
12, 4965–4996, 2015

for a specific year. $P_{\geq 10\,\mathrm{year}}$ was the summation of daily rainfall no less than 10 mm in a year and $P_{\geq 10\mathrm{annual}}$ was the annual average for $P_{\geq 10\,\mathrm{year}}$.

Models by Wang (1987) and Wang et al. (1995) utilized ($\mathrm{m\,t\,cm\,ha^{-1}\,h^{-1}\,a^{-1}}$) as the unit of R for comparison. A conversion factor of 10.2 was multiplied to convert R to $\mathrm{MJ\,mm\,ha^{-1}\,h^{-1}\,a^{-1}}$. Later, models by Wu (1994) and Zhou et al. (1995) utilized $J\,\mathrm{cm\,m^{-2}\,h^{-1}\,a^{-1}}$. Their conversion factor, 10, was multiplied to convert ($J\,\mathrm{cm\,m^{-2}\,h^{-1}\,a^{-1}}$) to ($\mathrm{MJ\,mm\,ha^{-1}\,h^{-1}\,a^{-1}}$).

2.5 Assessment of the models

After the 21 models in Table 2 were calibrated with the data from the 11 calibration stations, the performance for these models was assessed and compared with the performance of the previously published models listed in Table 3 using data from the seven validation stations. Symmetric mean absolute percentage error ($\mathrm{MAPE_{sym}}$) and the Nash–Sutcliffe model efficiency coefficient (ME) were utilized to reflect the deviation of the calculated values from the observation data. $\mathrm{MAPE_{sym}}$ is superior to MAPE, since it can correct the problem of MAPE's asymmetry and the possible influence by outliers (Makridakis and Hibon, 1995). $\mathrm{MAPE_{sym}}$ was calculated as follows (Armstrong, 1985):

$$\mathrm{MAPE_{sym}} = \frac{100}{m}\sum_{k=1}^{m}\left|\frac{R_{\mathrm{sim}}(k) - R_{\mathrm{obs}}(k)}{(R_{\mathrm{sim}}(k) + R_{\mathrm{obs}}(k))/2}\right| \quad (10)$$

where R_{obs} is the measured rainfall erosivity for the k^{th} period of time, such as monthly, yearly, or annual, based on one-minute resolution rainfall data. R_{sim} is the estimated value for the same period using equations in Tables 2 or 3.

HESSD
12, 4965–4996, 2015

ME was calculated as follows (Nash and Sutcliffe, 1970):

$$\mathrm{ME} = 1 - \frac{\sum_{k}^{m}[R_{\mathrm{sim}}(k) - R_{\mathrm{obs}}(k)]^2}{\sum_{k}^{m}[R_{\mathrm{obs}}(k) - \overline{R_{\mathrm{obs}}}(k)]^2} \quad (11)$$

ME compares the measured values on the line as a perfect fit (1 : 1 line). Hence, ME is a combined measure of linearity, bias, and relative differences between the measured and predicted values. The maximum possible value for ME is 1. The higher the value the better the model fit. An efficiency of ME < 0 indicates the single value (the mean) for the measured data's mean is a better predictor of the data than the model.

$\mathrm{MAPE}_{\mathrm{sym}}$ and ME were calculated station by station for seven validation stations and their mean values for all stations were reported. R_{obs} has only one value for each station for the annual average scale of R estimation, and hence ME was calculated based on simulations and observations for the seven stations.

3 Results and discussions

3.1 Basic data results

Average annual rainfall ranged from 449.7 to 1728.1 mm, and average annual erosivity varied from 781.9 to 8258.5 $\mathrm{MJ\,mm\,ha^{-1}\,h^{-1}\,yr^{-1}}$ (Table 1). A total of 11 801 erosive events were used in the study. The eleven stations had 6376 erosive events, which were used to calibrate the models, and the seven validation stations had 5425 erosive events.

HESSD
12, 4965–4996, 2015

3.2 Validation and calibration for the models that use different resolutions of input data

Parameters, $MAPE_{sym}$, ME, and coefficients of determination, r^2, for calibration models are shown in Table 4. Statistical tests showed data from all stations could not be pooled.

The r^2 for all event level models was greater than 0.92 (Table 4). The model Event IV, with a combination of event rainfall amount P_{event} and I_{30}, when I_{30} was divided into two categories, with a threshold of 15 mm h^{-1}, performed best (Table 4). The performance of Daily I with daily rainfall amount and $(I_{10})_{daily}$ was similar with that for Event I with event rainfall amount and I_{10} (Table 4).

The power law models for monthly, yearly, average monthly, and annual scales (Monthly I, Yearly I, Average Monthly I and Annual I), with only total rainfall amount as input had determination coefficients r^2 greater than 0.66, which suggested the models were statistically significant (Table 4 and Fig. 2). However, their capabilities in predicting R with time scales intended for the models were limited or ineffective, with ME being 0.20, −0.83, −0.44 and 0.63 for Monthly I, Yearly I, Average Monthly I and Annual I, respectively. Data from Tengchong and Xichang, located in the south-western part of China, were mainly responsible for the lower ME values. When these two stations were removed, the average ME for monthly scale of R increased to 0.59 for Monthly I, 0.37 for Yearly I, and 0.60 for Average Monthly I (Table 5). Seasonal variations by monthly and average monthly models (Fig. 3) and yearly variations by monthly and yearly models (Fig. 4) were demonstrated using Tonghe and Tengchong stations. Monthly I and Average Monthly I captured the general seasonal pattern for the Tonghe station (Fig. 3a and c), but the simulated peak value of monthly R was in July for the Tengchong station, which was not consistent with observation. Monthly I and Yearly I captured the general year-to-year pattern for the Tonghe station (Fig. 4a and c), but they overestimated yearly erosivity for the Tengchong station (Fig. 4b and d). Monthly I and Yearly I also overestimated the yearly erosivity for the Xichang station. The reason for the overestimation for the Tengchong and Xichang stations was

HESSD
12, 4965–4996, 2015

mainly due to two aspects: (1) the percentages of erosive rainfall amount to total rainfall at those stations were lower (71.9 and 76.9 %, respectively), suggesting that more events occurred with small amount totals that do not generate soil loss (Table 5); and (2) the ratio for event EI_{30} to event rainfall amount P was lower (3.6 and 4.1, respectively), inferring that rainfall intensity and erosivity generated by per amount of rainfall were both less than that of the other stations (Table 5). This result was consistent with that of Nel et al. (2013), which demonstrated that two models using annual average rainfall and average monthly rainfall substantially overestimated annual erosivity in the west coast and the Central Plateau of Mauritius, which also have a large amount of non-erosive rainfall. Rainfall erosivity reflected a combined effect of rainfall amount and rainfall intensity. Therefore, it was reasonable that rainfall amount could only explain part of rainfall erosivity variation at these stations.

Models that used some expression of maximum daily rainfall amount (Monthly III, Yearly III, Average Monthly III, Average Monthly V, Annual III, and Annual Model V) predicted the R factor better than those models with only total rainfall amount as input (Table 4). Models based on rainfall amount and maximum contiguous 60 min rainfall amounts (Monthly II, Yearly II, Average Monthly II, Average Monthly IV, Annual II, and Annual IV) generally performed better than corresponding models with rainfall amount and maximum daily rainfall amount (Monthly III, Yearly III, Average Monthly III, Average Monthly V, Annual III), except for Annual Model V, which performed well. The reason may be due to the fact that maximum contiguous 60 min rainfall amounts may have been more highly correlated with maximum contiguous 30 min intensity in an event as compared to just the maximum daily rainfall amount.

Taking Tonghe and Tengchong as examples, it was demonstrated that Monthly II generated better result than Monthly III, which performed better than Monthly I, in estimating seasonal and yearly variations (Figs. 3a, b and 4a, b). Correspondingly, seasonal variations by Average Monthly II were closer to observations as compared to those by Average Monthly III and Average Monthly I (Fig. 3c and d). Yearly II and Yearly III

HESSD
12, 4965–4996, 2015

improved the simulation of yearly variations compared with Yearly I, especially for the Tengchong station (Fig. 4c and d).

3.3 Comparisons with previous research

Wang et al. (1995) used a combination of event rainfall amount P_{event} and I_{10} for event scale models. The model using the I_{10} data was divided into two categories, with a threshold of 10 mm h^{-1}, performed best among the four models compared (Table 3). That model had similar performance with Event IV in this study (Table 4).

There are three kinds of daily scale models, according to the number and type of inputs required. Two models used daily rainfall amount (Zhang et al., 2002b and Xie et al., 2015), two models used daily rainfall amount and daily maximum 10 min intensity (Xie et al., 2001 and Daily I), and one model used daily rainfall amount and daily maximum 60 min intensity (Xie et al., 2015). The model with daily rainfall amount as input in Xie et al. (2015) performed better than that of Zhang et al. (2002b) (Table 3). Daily I, which used daily rainfall amount and daily maximum 10 min intensity as inputs in this study, performed better than the model in Xie et al., (2001). Models with an additional daily 10 min or 60 min intensity index performed better than those with only a rainfall amount index (Tables3 and 4).

There are generally four groups of models for monthly, yearly, average monthly, and annual scale models. The first group used linear regression (Sun et al., 1990; Wu, 1994; Zhou et al., 1995) or a power law function (Zhang and Fu, 2003; Monthly I, Yearly I, Average Monthly I, and Annual I) with rainfall amount as input so that the data required were relatively easy to collect. Models by Sun et al. (1990), Wu (1994) and Zhou et al. (1995), when they were used to estimate the monthly scale of R, had $MAPE_{sym}$ values of 88.3, 60.9 and 67.8 % and ME of −1.96, 0.53 and 0.38, respectively (Table 3). When they were used to estimate annual scale of R, there was a tendency of underestimation, especially for the stations with larger erosivity (Fig. 5a, b). Four models by Zhang and Fu (2003) overestimated the R factor, with $MAPE_{sym}$ varying between 34.6 and 60.8 % and ME varying between −2.41 to −0.03 (Table 3, Fig. 5), which sug-

HESSD
12, 4965–4996, 2015

gested the models' abilities were limited. Two models by Zhang and Fu (2003) using the Modified Fournier Index generated worse results compared to the model by Zhang and Fu (2003) using average annual rainfall as input (Table 3), which was consistent with the result of Yu and Rosewell (1996). The power law models in this study, including Monthly I, Yearly I, Average Monthly I, and Annual I, tended to overestimate the R factor for the stations with larger erosivity (Fig. 5).

The second group of models (Wang et al., 1995; Monthly II, Yearly II, Average Monthly IV, Annual IV) used linear regression with rainfall amount (total rainfall or total rainfall with daily rainfall no less than 10 mm) and maximum 60 min rainfall as inputs. All these seven models generated good results, with $MAPE_{sym}$ for R with time scale intended for the model ranging from 11.4 to 35.6 % and ME from 0.42 to 0.94 (Tables 3 and 4). When these models were used to estimate annual R, the measured and predicted values were near the 1 : 1 line (Fig. 5).

The third group used linear regression with rainfall amount and maximum daily rainfall as inputs (Monthly III, Yearly III, Average Monthly V, Annual V), which generated reasonable results (Table 4) and a slightly overestimated annual R (Fig. 5). Overall they did not perform as well as the models in the second group (Table 4).

The fourth group (Wang et al., 1995) used a combination of three indices, including rainfall amount, maximum 60 min rainfall amount, and maximum daily rainfall amount as inputs and generated good simulation results, however, there was no improvement compared with the two models by Wang et al. (1995) in the second group.

3.4 Uncertainty for the models at different time scales of the *R* factor

Generally speaking, the more accurate the resolution of input data for models, the better was the performance of the model. For example, the models with daily rainfall amount and daily maximum 60 or 10 min amount as inputs performed better than models with daily rainfall amount as input. Results from models with maximum 60 min rainfall amount (Monthly II, Yearly II, Average Monthly IV, and Annual IV) were generally

HESSD
12, 4965–4996, 2015

better than those with maximum daily rainfall amount (Monthly III, Yearly III, Average Monthly V, and Annual V, Fig. 5).

If monthly rainfall data are available, there are several models from which to choose. For example, if only monthly rainfall amounts are available, Monthly I, Yearly I, Average Monthly I, and Annual I can be selected. Yearly, average monthly, and annual rainfall amounts can be first derived from monthly rainfall amount data and then used in the corresponding models to estimate the *R* factor. The prediction capabilities for seven validation stations for the four models; Monthly I, Yearly I, Average Monthly I, and Annual I, were very similar to each other (Table 5, Fig. 5). Similar results can be found among four models with maximum 60 min amount, including Monthly II, Yearly II, Average Monthly IV, and Annual IV, as well as the four models with maximum daily rainfall amount, including Monthly III, Yearly III, Average Monthly V, and Annual Model V. Therefore, users have the option to choose the simplest method for estimating the *R* factor. However, if seasonal variations are required, monthly and average monthly models may be utilized; whereas, yearly and annual models cannot satisfy the requirements. If yearly variations are required, monthly and yearly models may be utilized; whereas, average monthly, and annual models cannot satisfy the requirements.

4 Conclusions

Rainfall erosivity is needed for using USLE-type soil erosion models. Considering the difficulties in obtaining breakpoint data to calculate the erosivity index, a series of 21 simpler methods using different resolutions of often readily available rainfall data were calibrated, based on 6376 erosive events derived from one-minute resolution data from 11 stations. These models, plus 20 models from previous research, were evaluated by using 5425 erosive events from the seven validation stations. The following conclusions are presented:

HESSD
12, 4965–4996, 2015

1. Symmetric mean absolute percentage error ($MAPE_{sym}$) and the Nash–Sutcliffe model efficiency coefficient (ME) were presented for 41 models to reflect deviation of the simulation from the observation when different time scales for the *R* factor were estimated, including event/daily, monthly, yearly, average monthly, and annual scales. Models in this study performed better or similar with models from previous research.

2. Predication capabilities for models with rainfall amount as inputs were limited in the geographic region of southwestern China, where the percent of erosive amount was lower and the ratio for event EI_{30} to event rainfall amount *P* was lower.

3. Models with higher temporal resolution of input generally performed better. Models with rainfall amount and maximum 60 min rainfall amount as inputs performed better than models with rainfall amount and maximum daily rainfall amount, which performed better than those with only rainfall amount. Users can select different models to calculate rainfall erosivity, based on their available rainfall data and objectives. For example, if the user wants to estimate event scale EI_{30}, then they must choose an event model. However, if the objective is estimating average annual R, then there are many choices of models that use various resolutions of input rainfall data.

In summary, from the view of prediction accuracy, the event EI_{30} as originally calculated is considered the best indicator of rainfall erosivity for either erosivity distribution analysis or annual erosivity calculation. However, in the absence of breakpoint rainfall data users can select from the different methods presented here to calculate rainfall erosivity, based on availability of rainfall data and accuracy requirements.

Acknowledgements. The authors would like to thank the Heilongjiang, Shanxi, Shaanxi, Beijing, Sichuan, Hubei, Fujian, and Yunnan Meteorological Bureaus for supplying rainfall data. This work was supported by the National Natural Science Foundation of China (No. 41301281) and the China Scholarship Council. USDA is an equal opportunity provider and employer.

HESSD
12, 4965–4996, 2015

References

Angel, J. R., Palecki, M. A., and Hollinger, S. E.: Storm precipitation in the United States, Part II: Soil erosion characteristics, J. Appl. Meteorol., 44, 947–959, 2005.

Angulo-Martinez, M. and Begueria, S.: Trends in rainfall erosivity in NE Spain at annual, seasonal and daily scales, 1955–2006, Hydrol. Earth Syst. Sc., 16, 3551–3559, 2012.

Armstrong, J. S.: Long-range Forecasting: From Crystal Ball to Computer, 2nd edn., Wiley, New York, 1985.

Arnoldus, H. M. J.: Methodology used to determine the maximum potential average annual soil loss due to sheet and rill erosion in Morocco, FAO Soils Bull., 34, 39–51, 1977.

Bonilla, C. A. and Vidal, K. L.: Rainfall erosivity in Central Chile, J. Hydrol., 410, 126–133, 2011.

Capolongo, D., Diodato, N., Mannaerts, C. M., Piccarreta, M., and Strobl, R. O.: Analyzing temporal changes in climate erosivity using a simplified rainfall erosivity model in Basilicata (southern Italy), J. Hydrol., 356, 119–130, 2008.

China Meteorological Administration (CMA): Specifications for Surface Meteorological Observation, Meteorology Publishing House, Beijing, 2003.

Ferro, V., Porto, P., and Yu, B.: A comparative study of rainfall erosivity estimation for southern Italy and southeastern Australia, Hydrolog. Sci. J., 44, 3–24, 1999.

Fiener, P., Neuhaus, P., and Botschek, J.: Long-term trends in rainfall erosivity–analysis of high resolution precipitation time series (1937–2007) from Western Germany, Agr. Forest Meteorol., 171, 115–123, 2013.

Foster, G. R.: User's Reference Guide: Revised Universal Soil Loss Equation (RUSLE2), US Department of Agriculture, Agricultural Research Service, Washington, D. C., 2004.

Huang, Y. H., Lu, C. L., Zheng, T. F., Fu, Q., and Xu, J. J.: Rainfall erosivity index in southeastern Fujian, J. Soil Water Conserv., 6, 1–5, 1992.

Kinnell, P. I. A.: AGNPS-UM: Applying the USLE-M within the agricultural non-point source pollution model, Environ. Modell. Softw., 15, 331–341, 2000.

Liu, B. Y., Zhang, K. L., and Xie, Y.: An empirical soil loss equation. in: Proceedings–Process of soil erosion and its environment effect (Vol. II), 12th international soil conservation organization conference, Tsinghua University Press, Beijing, 21–25, 2002.

Liu, B. Y., Guo, S. Y., Li, Z. G., Xie, Y., Zhang, K. L., and Liu, X. C.: Water erosion sample survey in China, Soil Water Conserv. China, 10, 26–34, 2013.

HESSD
12, 4965–4996, 2015

Lo, A., El-Swaify, S. A., Dangler, E. W., and Shinshiro, L.: Effectiveness of EI_{30} as an erosivity index in Hawaii, in: Soil Erosion and Conservation, edited by: El-Swaify, S. A., Moldenhauer, W. C., and Lo, A., Soil Conservation Society of America, Ankeny, 384–392, 1985.
Ma, X., He, Y. D., Xu, J. C., Noordwijk, M. V., and Lu, X. X.: Spatial and temporal variation in rainfall erosivity in a Himalayan watershed, Catena, 121, 248–259, 2014.
Makridakis, S. and Hibon, M.: Evaluating accuracy (or error) measures, Working paper, INSEAD, Fontainebleau, France, 1995.
Nash, J. E. and Sutcliffe, J. V.: River flow forecasting through conceptual models, Part 1: A discussion of principles, J. Hydrol., 10, 282–290, 1970.
Nearing, M. A.: Potential changes in rainfall erosivity in the United States with climate change during the 21st century, J. Soil Water Conserv., 56, 229–232, 2001.
Nel, W., Anderson, R. L., Sumner, P. D., Boojhawon, R., Rughooputh, S. D. D. V., and Dunputh, B. H. J.: Temporal sensitivity analysis of erosivity estimations in a high rainfall tropical island environment, Geogr. Ann. A, 95, 337–343, 2013.
Plangoen, P. and Babel, M. S.: Projected rainfall erosivity changes under future climate in the upper Nan watershed, Thailand, J. Earth Sci. Clim. Change, 5, 242, doi:10.4172/2157-7617.1000242, 2014.
Ramos, M. C. and Duran, B.: Assessment of rainfall erosivity and its spatial and temporal variabilities: case study of the Penedès area (NE Spain), Catena, 123, 135–147, 2014.
Renard, K. G and Freimund, J. R.: Using monthly precipitation data to estimate the *R*-factor in the revised USLE, J. Hydrol., 15, 287–306, 1994.
Renard, K. G., Foster, G. R., Weesies, G. A., McCool, D. K., and Yoder, D. C.: Predicting soil erosion by water, in: Agriculture Handbook 703, US Department of Agriculture, Agricultural Research Service, Washington DC, 1997.
Richardson, C. W., Foster, G. R., and Wright, D. A.: Estimation of erosion index from daily rainfall amount, T. ASAE, 26, 153–156, 1983.
Sanchez-Moreno, J. F., Mannaerts, C. M., and Jetten, V.: Rainfall erosivity mapping for Santiago island, Cape Verde, Geoderma, 217, 74–82, 2014.
Segura, C., Sun, G., McNulty, S., and Zhang, Y.: Potential impacts of climate change on soil erosion vulnerability across the conterminous United States, J. Soil Water Conserv., 69, 171–181, 2014.
Shiono, T., Ogawa, S., Miyamoto, T., and Kameyama, K.: Expected impacts of climate change on rainfall erosivity of farmlands in Japan, Ecol. Eng., 61, 678–689, 2013.

HESSD
12, 4965–4996, 2015

Snedecor, G. W. and Cochran, W. G.: Statistical Methods, 12th edn, The Iowa State University Press, Ames, 1989.
Sun, B. P., Zhao, Y. N., and Qi, S.: Application of USLE in loessial gully hill area, Memoir of NISWC, Academia Sinica and Ministry of Water Conservancy, Yangling, 12, 50–59, 1990.
Sun, J. H., Zhu, Q. D., Yan, Z. J., Lu H. M., and Wang H. R.: A review of research and application of AGNPS model, Adv. Water Resour., 20, 876–884, 2009.
Verstraeten, G., Poesen, J., Demaree, G., and Salles, C.: Long-term (105 years) variability in rain erosivity as derived from 10 min rainfall depth data for Ukkel (Brussels, Belgium): implications for assessing soil erosion rates, J. Geophys. Res., 111, D22109, doi:10.1029/2006JD007169, 2006.
Wang, B. M., Lu, Y. P., and Zhang, Q.: The color scanning digitizing processing system of precipitation autographic record paper, J. Appl. Meteorol., 15, 737–744, 2004.
Wang, W. Z.: Index of ranfall erosivity (r) in loess area, J. Soil Water Conserv., 12, 34–40, 1987.
Wang, W. Z., Jiao, J. Y., and Hao, X. P.: Distribution of rainfall erosivity *R* value in China, J. Soil Water Conserv., 9, 5–18, 1995.
Wischmeier, W. H.: Use and misuse of the universal soil loss equation, J. Soil Water Conserv., 31, 5–9, 1976.
Wischmeier, W. H. and Smith, D. D.: Rainfall energy and its relationship to soil loss, Eos T. Am. Geophys. Un., 39, 285–291, 1958.
Wischmeier, W. H. and Smith, D. D.: Predicting rainfall-erosion losses from cropland east of the Rocky Mountains, Agriculture Handbook 282, US Department of Agricultural Research Service, Washington DC, 1965.
Wischmeier, W. H. and Smith, D. D.: Predicting rainfall erosion losses: a guide to conservation planning, Agriculture Handbook 537, US Department of Agricultural, Agricultural Research Service, Washington DC, 1978.
Wu, S. Y.: Simplified method on calculation of runoff erosion force in Dabieshan mountainous area and its temporal and spatial distribution, J. Soil Water Conserv., 4, 12–13, 1994.
Xie, Y., Zhang, W. B., and Liu, B. Y.: Rainfall erosivity estimation using daily rainfall amount and intensity, Bull. Soil Water Conserv., 6, 53–56, 2001.
Xie, Y., Liu, B. Y., and Nearing, M. A.: Practical thresholds for separating erosive and non-erosive storms, T. ASAE, 45, 1843–1847, 2002.
Xie, Y., Yin, S. Q., Liu, B. Y., Nearing, A. M., and Zhao, Y.: Daily rainfall erosivity model development in China, J. Hydrol., submitted, 2015.

HESSD
12, 4965–4996, 2015

Yin, S. Q., Xie, Y., Nearing, M. A., Wang, C. G.: Estimation of rainfall erosivity using 5 to 60 min fixed-interval rainfall data from China, Catena, 70, 306–312, 2007.
Yu, B.: Rainfall erosivity and its estimation for Australia's tropics, Aust. J. Soil Res., 36, 143–165, 1998.
Yu, B. and Rosewell, C. J.: A robust estimator of the R-factor for the universal soil loss equation, T. ASAE, 39, 559–561, 1996.
Zhang, W. B. and Fu, J. S.: Rainfall erosivity estimation under different rainfall amount, Resour. Sci., 25, 35–41, 2003.
Zhang, W. B., Xie, Y., and Liu, B. Y.: Estimation of rainfall erosivity using rainfall amount and rainfall intensity, Geogr. Res., 21, 384–390, 2002a.
Zhang, W. B., Xie, Y., and Liu, B. Y.: Rainfall erosivity estimation using daily rainfall amounts, Sci. Geogr. Sin., 22, 705–711, 2002b.
Zhang, Y. G., Nearing, M. A., Zhang, X. C., Xie, Y., and Wei, H.: Projected rainfall erosivity changes under climate change from multimodel and multiscenario projections in Northeast China, J. Hydrol., 384, 97–106, 2010.
Zhou, F. J., Chen, M. H., and Lin, F. X.: The rainfall erosivity index in Fujian province, J. Soil Water Conserv., 9, 13–18, 1995.

HESSD
12, 4965–4996, 2015

Table 1. Information for the 18 rainfall stations.

Province	Station name	Lat. (° N)	Long. (° E)	Elevation (m)	Effective years	No. of erosive events	Annual rainfall[3] (mm)	R[4] (MJ mm ha^{-1} h^{-1} a^{-1})
Heilongjiang[1]	Nenjiang	49.17	125.23	243.0	30	343	485.8	1368.7
	Tonghe[2]	45.97	128.73	110.0	38	471	596.2	1632.5
Shanxi[1]	Wuzhai	38.92	111.82	1402.0	30	289	464.0	781.9
	Yangcheng[2]	35.48	112.4	658.8	30	340	605.9	1503.3
Shaanxi[1]	Suide	37.5	110.22	928.5	29	256	449.7	992.8
	Yan'an	36.6	109.5	958.8	39	411	534.6	1233.7
Beijing[1]	Guanxiangtai	39.93	116.28	54.7	40	434	575.0	3188.1
	Miyun[2]	40.38	116.87	73.1	37	476	648.1	3575.0
Sichuan	Chengdu	30.67	104.02	506.1	39	717	891.8	3977.0
	Xichang[2]	27.9	102.27	1590.9	40	998	1007.5	3021.0
	Suining	30.5	105.58	279.5	33	654	932.7	4091.3
	Neijiang	29.58	105.05	352.4	39	826	1034.1	5097.9
Hubei	Fangxian	32.03	110.77	427.1	31	563	829.5	2298.4
	Huangshi[2]	30.25	115.05	20.6	32	898	1438.5	6049.4
Yunnan	Tengchong[2]	25.02	98.5	1648.7	36	1205	1495.7	3648.9
	Kunming	25.02	102.68	1896.8	33	747	1018.8	3479.0
Fujian	Fuzhou	26.08	119.28	84.0	39	1136	1365.4	5871.1
	Changting[2]	25.85	116.37	311.2	31	1037	1728.1	8258.5

[1] The eight stations in these provinces are located in the northern part of China and had one-minute resolution data collected from May through September. The remaining ten stations were based on data collected during the entire year.
[2] Seven validation stations (The other 11 stations were calibration stations.)
[3] Based on daily rainfall datasets collected during 1961–2000.
[4] R in this case is the average annual erosivity.

HESSD
12, 4965–4996, 2015

Table 2. Models calibrated.

Model codes	Models	Model codes	Models
Event I	$EI_{30} = \lambda_1 P_{event} I_{10}$	Average Monthly I	$R_{ave\_month} = \alpha_3 P_{ave\_month}^{\beta_3}$
Event II	$EI_{30} = \lambda_2 P_{event} I_{30}$	Average Monthly II	$R_{ave\_month} = \lambda_{11} P_{ave\_month} (P_{60})_{month\_max}$
Event III	$EI_{30} = \lambda_3 P_{event} I_{60}$	Average Monthly III	$R_{ave\_month} = \lambda_{12} P_{ave\_month} \overline{(P_{1440})_{month\_max}}$
Event IV	$EI_{30} = \lambda_4 P_{event} I_{30}$ $I_{30} < 15\,mm\,h^{-1}$ $EI_{30} = \lambda_5 P_{event} I_{30}$ $I_{30} \geq 15\,mm\,h^{-1}$	Average Monthly IV	$R_{ave\_month} = \lambda_{13} P_{ave\_month} \overline{(P_{60})_{month}}$
Daily I	$R_{day} = \lambda_6 P_{day} (I_{10})_{day}$	Average Monthly V	$R_{ave\_month} = \lambda_{14} P_{ave\_month} \overline{(P_{1440})_{month}}$
Monthly I	$R_{month} = \alpha_1 P_{month}^{\beta 1}$	Annual I*	$R_{annual} = \alpha_4 P_{annual}^{\beta_4}$
Monthly II	$R_{month} = \lambda_7 P_{month} (P_{60})_{month}$	Annual II	$R_{annual} = \lambda_{15} P_{annual} (P_{60})_{year\_max}$
Monthly III	$R_{month} = \lambda_8 P_{month} (P_{1440})_{month}$	Annual III	$R_{annual} = \lambda_{16} P_{annual} \overline{(P_{1440})_{year\_max}}$
Yearly I	$R_{year} = \alpha_2 P_{year}^{\beta_2}$	Annual IV	$R_{annual} = \lambda_{17} P_{annual} \overline{(P_{60})_{annual}}$
Yearly II	$R_{year} = \lambda_9 P_{year} (P_{60})_{year}$	Annual V	$R_{annual} = \lambda_{18} P_{annual} (P_{1440})_{annual}$
Yearly III	$R_{year} = \lambda_{10} P_{year} (P_{1440})_{year}$		

* Annual refers to Average Annual values of erosivity.

HESSD
12, 4965–4996, 2015

Table 3. Models published in previous research and their prediction capabilities determined using symmetric mean absolute percentage errors and Nash–Sutcliffe model efficiency coefficients.

Erosivity time scales	Models	Sources	$MAPE_{sym}$ (%)[1]	ME^2
Event	$EI_{30} = 10.2 \cdot (0.0247 P_{event} I_{30} - 0.17)$	Wang (1987)	30.2	0.96
	$EI_{30} = 10.2 \cdot (0.025 P_{event} I_{30} - 0.32)$	Wang (1987)	28.4	0.95
	$EI_{30} = 10.2 \cdot \left(1.70 \frac{P_{event} I_{30}}{100} - 0.136\right) \quad I_{30} < 10\,mm\,h^{-1}$			
	$EI_{30} = 10.2 \cdot \left(2.35 \frac{P_{event} I_{30}}{100} - 0.523\right) \quad I_{30} \geq 10\,mm\,h^{-1}$	Wang et al. (1995)	15.4	0.97
	$EI_{30} = 0.1773 P_{event} I_{10}$	Zhang et al. (2002a)	44.3	0.85
Daily	$R_{day} = 0.184 P_{day} (I_{10})_{day}$	Xie et al. (2001)	44.6	0.88
	$R_{day} = \alpha P_{day}^{\beta}$			
	$\beta = 0.8363 + \frac{18.144}{P_{d12}} + \frac{24.455}{P_{y12}}, \alpha = 21.586\beta^{-7.1891}$	Zhang et al. (2002b)	73.8	0.52
	$R_{day} = 0.2686[1 + 0.5412 \cos(\frac{\pi}{6} j - \frac{7\pi}{6})] P_{day}^{1.7265}$	Xie et al. (2015)	65.8	0.58
	$R_{day} = 0.3522 P_{day} (P_{60})_{day}$	Xie et al. (2015)	38.4	0.93
Monthly	$R_{month} = 10 \cdot 0.0125 P_{month}^{1.6295}$	Wu (1994)	60.9	0.53
	$R_{month} = 10 \cdot (0.3046 P_{month} - 2.6398)$	Zhou et al. (1995)	67.8	0.39
Yearly	$R_{year} = 1.77 P_{5-10} - 133.03$	Sun et al. (1990)	88.3	−1.96
	$R_{year} = 10.2 \cdot 0.272 (P_{year} (P_{60})_{year} / 100)^{1.205}$	Wang et al. (1995)	32.0	0.42
	$R_{year} = 10.2 \cdot 1.67 (P_{\geq 10\,year} (P_{60})_{year} / 100)^{0.953}$	Wang et al. (1995)	18.8	0.69
	$R_{year} = 0.0534 P_{year}^{1.6548}$	Zhang and Fu (2003)	43.5	−2.41
Average Annual	$R_{annual} = 10.2 \cdot 0.009 P_{annual}^{0.564} \cdot \overline{(P_{60})_{annual}}^{1.155} \cdot \overline{(P_{1440})_{annual}}^{0.560}$	Wang et al. (1995)	17.3	0.83
	$R_{annual} = 10.2 \cdot 0.0244 P_{\geq 10 annual}^{0.551} \cdot \overline{(P_{60})_{annual}}^{1.175} \cdot \overline{(P_{1440})_{annual}}^{0.376}$	Wang et al. (1995)	12.0	0.86
	$R_{annual} = 10.2 \cdot 2.135 (P_{\geq 10 annual} \cdot (P_{60})_{annual} / 100)^{0.919}$	Wang et al. (1995)	11.4	0.94
	$R_{annual} = 0.1833 F_F^{1.9957}, F_F = \frac{1}{N} \sum_{i=1}^{N} \frac{\sum_{j=1}^{12} P_{i,j}^2}{\sum_{j=1}^{12} P_{i,j}}$	Zhang and Fu (2003)	55.9	−1.21
	$R_{annual} = 0.3589 F^{1.9462}, F = \left(\sum_{j=1}^{12} P_{ave\_month\_j}^2\right) / P_{annual}$	Zhang and Fu (2003)	60.8	−2.11
	$R_{annual} = 0.0668 P_{annual}^{1.6266}$	Zhang and Fu (2003)	34.6	−0.03

[1] $MAPE_{sym}$ (%) is symmetric mean absolute percentage error for R with time scale intended for the model to reflect the deviation of the simulation from the observation. For example, if the erosivity time scale for the model was monthly, the simulation and observation were monthly R values. $MAPE_{sym}$ was calculated station by station for seven validation stations, respectively and the mean values for all seven stations were presented here.

[2] ME is the Nash–Sutcliffe model efficiency coefficient for R with time scale intended for the model. ME was calculated based on simulations and observations for seven stations for the annual average scale of R estimation and was averaged for all seven stations for the other scales.

HESSD
12, 4965–4996, 2015

Table 4. Models calibrated in this study and their prediction capabilities determined using symmetric mean absolute percentage errors and Nash–Sutcliffe model efficiency coefficients.

Model codes	Models[1]	r^2 [2]	$MAPE_{sym}$ (%)	ME
Event I	$EI_{30} = 0.1547 P_{event} I_{10}$	0.92	34.4	0.90
Event II	$EI_{30} = 0.2372 P_{event} I_{30}$	0.98	29.0	0.97
Event III	$EI_{30} = 0.3320 P_{event} I_{60}$	0.94	36.0	0.93
Event IV	$EI_{30} = 0.1592 P_{event} I_{30} \quad I_{30} < 15\,mm\,h^{-1}$ $EI_{30} = 0.2394 P_{event} I_{30} \quad I_{30} \geq 15\,mm\,h^{-1}$	0.97	13.8	0.97
Daily I	$R_{day} = 0.1661 P_{day} (I_{10})_{day}$	0.92	38.1	0.90
Monthly I	$R_{month} = 0.1575 P_{month}^{1.6670}$	0.66	68.1	0.20
Monthly II	$R_{month} = 0.1862 P_{month} (P_{60})_{month}$	0.85	35.6	0.83
Monthly III	$R_{month} = 0.0770 P_{month} (P_{1440})_{month}$	0.65	55.8	0.59
Yearly I	$R_{year} = 0.5115 P_{year}^{1.3163}$	0.70	37.2	−0.83
Yearly II	$R_{year} = 0.1101 P_{year} (P_{60})_{year}$	0.80	20.7	0.56
Yearly III	$R_{year} = 0.0502 P_{year} (P_{1440})_{year}$	0.54	28.8	0.11
Average Monthly I	$R_{ave\_month} = 0.0755 P_{ave\_month}^{1.8430}$	0.89	41.5	−0.44
Average Monthly II	$R_{ave\_month} = 0.0877 P_{ave\_month} (P_{60})_{month\_max}$	0.94	22.9	0.82
Average Monthly III	$R_{ave\_month} = 0.0410 P_{ave\_month} (P_{1440})_{month\_max}$	0.87	29.8	0.72
Average Monthly IV	$R_{ave\_month} = 0.2240 P_{ave\_month} \overline{(P_{60})_{month}}$	0.98	20.8	0.81
Average Monthly V	$R_{ave\_month} = 0.1082 P_{ave\_month} \overline{(P_{1440})_{month}}$	0.94	29.1	0.74
Annual I	$R_{annual} = 1.2718 P_{annual}^{1.1801}$	0.89	25.6	0.63
Annual II	$R_{annual} = 0.0584 P_{annual} (P_{60})_{year\_max}$	0.92	15.4	0.91
Annual III	$R_{annual} = 0.0253 P_{annual} (P_{1440})_{year\_max}$	0.92	22.5	−0.44
Annual IV	$R_{annual} = 0.1058 P_{annual} \overline{(P_{60})_{annual}}$	0.94	17.0	0.88
Annual V	$R_{annual} = 0.0492 P_{annual} \overline{(P_{1440})_{annual}}$	0.92	18.2	0.91

[1] Parameters of models for power law models, including α_1, β_1, α_2, β_2, α_3, β_3, α_4, β_4, α_5, β_5, were solved by pooling data from 11 stations together. Parameters for average annual scale models, including λ_{15}, λ_{16}, λ_{17}, λ_{18}, were calculated by fitting data from all calibration stations and for the remainder they were the average values of parameters for the 11 calibration stations.
[2] r^2 is the coefficient of determination.

HESSD
12, 4965–4996, 2015

Table 5. Symmetric mean absolute percentage errors ($MAPE_{sym}$) and Nash–Sutcliffe model efficiency coefficients (ME) for R_{month} by Monthly I, R_{year} by Yearly I and R_{ave_month} by Average Monthly I models for seven validation stations and statistics on event rainfall amount and event EI_{30}.

Station name	R_{month} by Monthly I		R_{year} by Yearly I		R_{ave_month} by Average Monthly I		Percent of erosive amount (%)	EI_{30}/P
	$MAPE_{sym}$	ME	$MAPE_{sym}$	ME	$MAPE_{sym}$	ME		
Tonghe	70.2	0.73	30.9	0.47	29.5	0.93	71.2	4.8
Yangcheng	65.5	0.31	27.1	0.55	16.4	0.96	81.7	4.2
Miyun	52.0	0.71	45.1	−0.06	37.6	0.88	82.8	7.8
Xichang	77.5	0.47	45.4	−0.15	57.2	0.09	76.9	4.1
Huangshi	70.1	0.65	24.5	0.63	46.1	0.73	86.5	5.7
Tengchong	83.4	−2.01	66.6	−7.51	68.3	−6.98	71.9	3.6
Changting	52.0	0.54	20.9	0.26	35.2	0.30	88.4	6.1
Mean[1]	67.2	0.20	37.2	−0.83	41.5	−0.44	79.9	5.2
Mean[2]	62.0	0.59	29.7	0.37	38.7	0.60	82.1	5.7

[1] Averaged value for seven validation stations.
[2] Averaged value for five validation stations except Xichang and Tengchong.

HESSD
12, 4965–4996, 2015

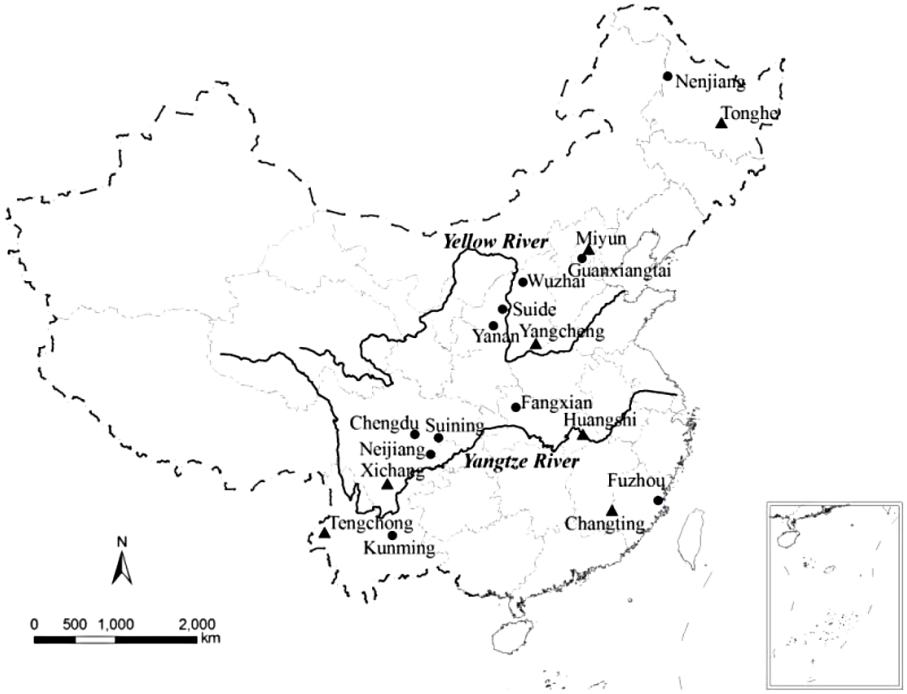

Figure 1. Distribution of the 18 stations with one-minute resolution rainfall data. Eleven stations marked with dots were used to calibrate 21 models. The other seven stations marked with triangles were used to validate models and conduct comparisons with previous research.

HESSD
12, 4965–4996, 2015

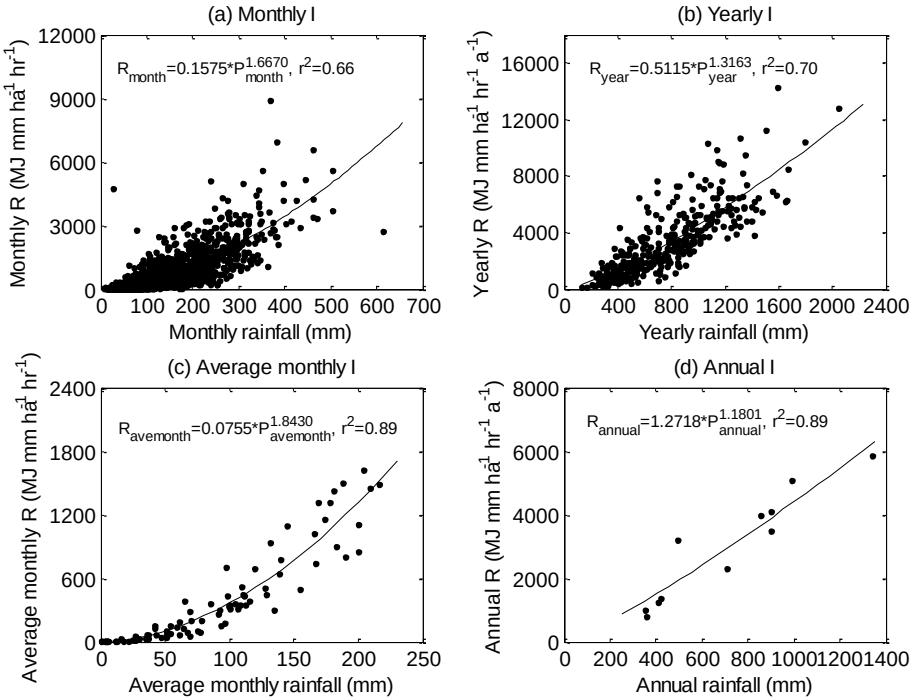

Figure 2. Scatterplots for power law models using rainfall amount: **(a)** Monthly I, **(b)** Yearly I, **(c)** Average Monthly I, and **(d)** Annual I, based on the 11 calibration stations.

HESSD
12, 4965–4996, 2015

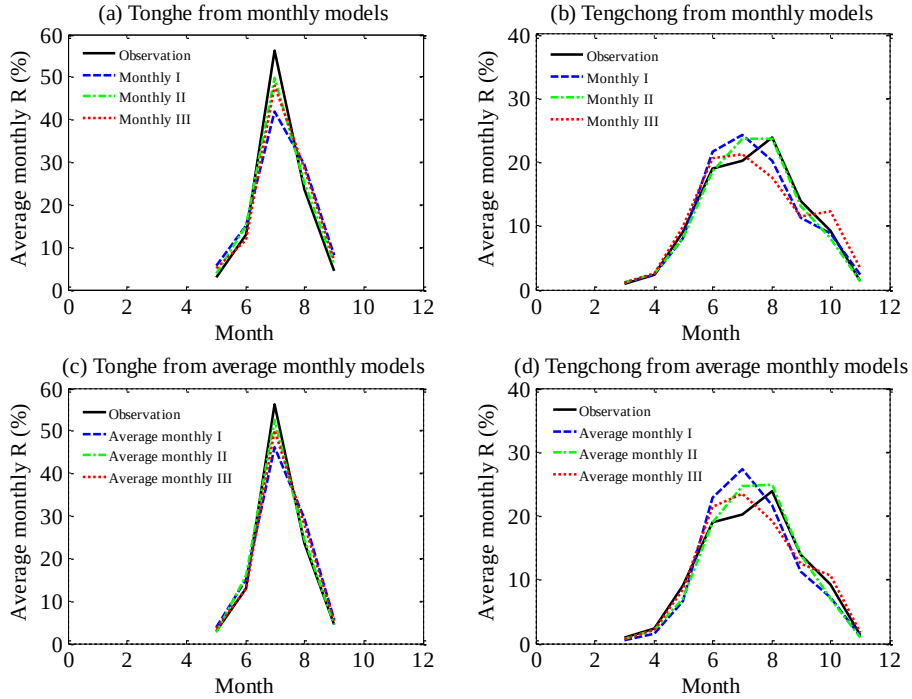

Figure 3. Comparisons of average monthly *R* values between observation values calculated using one-minute resolution rainfall data and estimated values using monthly models **(a, b)** and average monthly models **(c, d)** for the Tonghe and Tengchong stations.

HESSD
12, 4965–4996, 2015

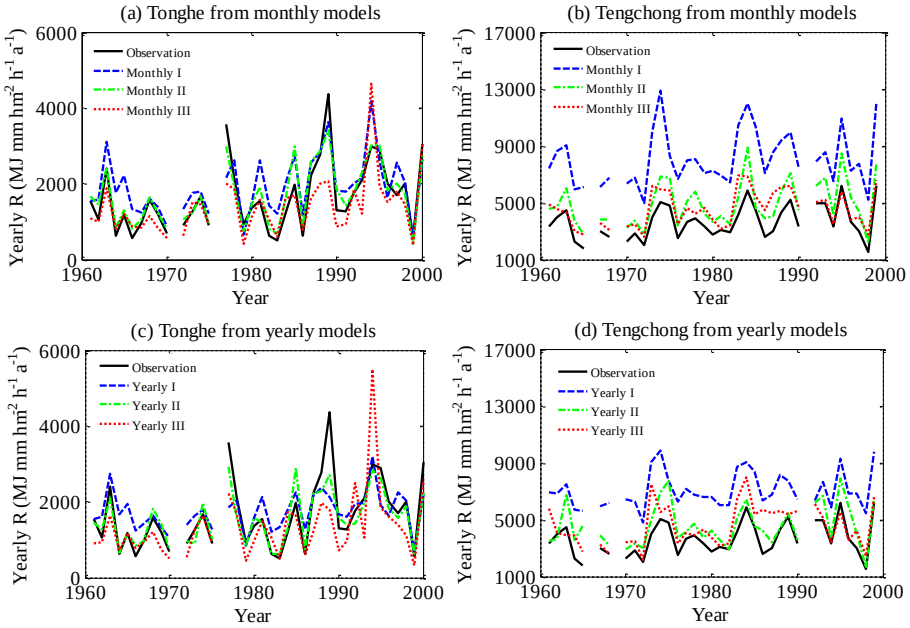

Figure 4. Comparison of yearly *R* values between observation values calculated using one-minute resolution rainfall data and estimated values using monthly models **(a, b)** and yearly models **(c, d)** for the Tonghe and Tengchong stations. The years without marks were ineffective years.

HESSD
12, 4965–4996, 2015

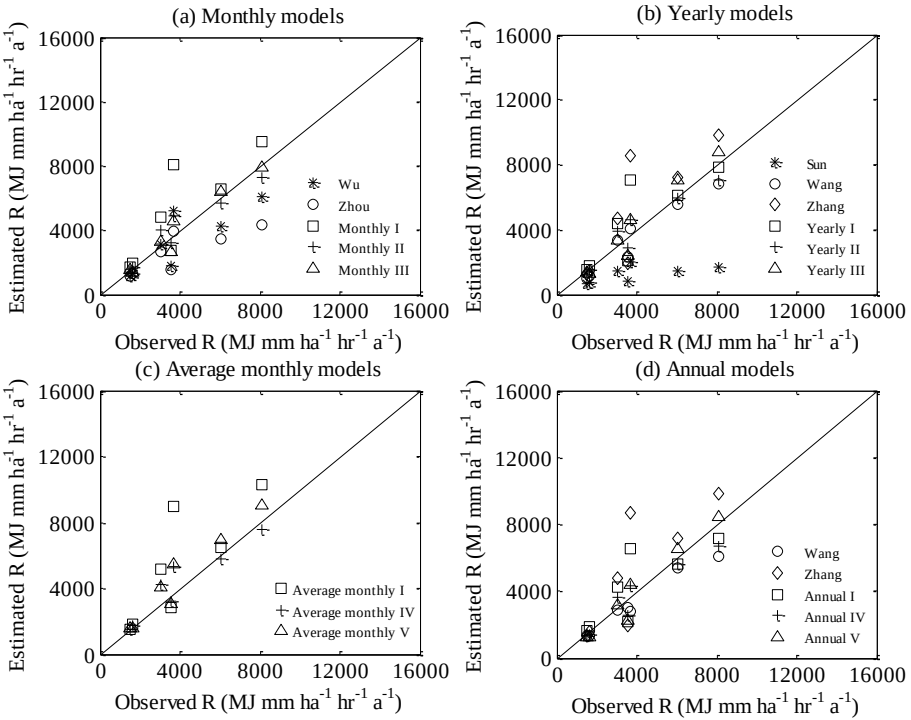

Figure 5. Comparisons of the estimated *R* factor value calculated based on **(a)** monthly, **(b)** yearly, **(c)** average monthly, and **(d)** average annual models using one-minute resolution data for seven independent validation stations. Monthly models included models in Wu (1994), Zhou et al. (1995), and Monthly I, II, and III from this study. Yearly models included models from Sun et al. (1990), Wang et al. (1995, the one with $MAPE_{sym}$ of 18.8 %), Zhang and Fu (2003), and Yearly I, II, and III from this study. Average monthly models included models from Average Monthly I, II, and III from this study. Average annual models included models from Wang et al. (1995, the one with $MAPE_{sym}$ of 11.4 %), Zhang and Fu (2003, the one with $MAPE_{sym}$ of 34.6 %), and Annual I, II, and III from this study.

HESSD
12, 4965–4996, 2015